

ANALYSIS OF PARTICLE SEPARATION WITH RESPECT TO PRE-IGNITION IN AN SI-ENGINE

MICHAEL HEISS^{*}, THOMAS LAUER^{*}

^{*} Vienna University of Technology
Institute for Powertrains and Automotive Technology
Getreidemarkt 9
1060 Vienna
AUSTRIA
Mail: michael.heiss@ifa.tuwien.ac.at
thomas.lauer@ifa.tuwien.ac.at
URL: www.ifa.tuwien.ac.at

Key Words: *Pre-Ignition, Multi-Component Fuel, Autoignition, Wall Film Formation, Particles, Lagrange*

Abstract

For downsized SI-engines at high loads and particularly at low engine speeds spontaneous self-ignitions randomly occur already before the regular spark timing leading to severe engine damage. This kind of irregular combustion phenomenon avoids fully exploiting the downsizing potential. Therefore, it was subject of extensive numerical and experimental investigations at the Institute for Powertrains and Automotive Technology at the Vienna University of Technology.

For the experimental investigations, a fuel with a high amount of components with low volatility and high boiling temperature was used to provoke wall film formation and droplet separation. An optical access was installed on the test engine for high-speed imaging. A five component model fuel was introduced in STAR-CD to reproduce a realistic evaporation and wall film behaviour in the CFD-simulations. Transient trajectories of separated droplets were compared to the path of recorded local light emissions. Especially stripped droplets from wetted areas on the piston crown close to the liner showed a good correlation with the video observations.

Additionally, the detachment of soot particles from the combustion chamber walls caused by the high-frequency pressure oscillations during a pre-igniting cycle was modelled in CFD with respect to the video observations. Particles that remained in the combustion chamber after gas exchange heated up during the following regular combustion cycle and therefore became critical for follow-up pre-ignition events in the next cycle.

In this way, droplets and particles could be confirmed as possible initiation mechanisms for pre-ignition.

1 INTRODUCTION

CO₂ emissions from anthropogenic sources are suspected to have an impact on the global warming. Governments around the globe react by defining targets for the reduction of greenhouse gases and CO₂ fleet emission. This is particularly a challenge for vehicles that are propelled by gasoline engines. A step towards a more efficient working process is the downsizing of gasoline engines using high boost pressures and direct injection. It allows the shifting of operating points to higher engine loads with higher efficiency.

However, experiences with highly boosted engines showed that at high loads and particularly at low engine speeds spontaneous self-ignitions randomly occur before the regular spark timing followed by a megaknock that may lead to engine damage in serious cases. Recent experimental studies revealed that oil/fuel droplets or deposits are a possible source of pre-ignition [1-3].

It is the aim of the presented work to analyse the mechanisms that initiate pre-ignition using different measuring techniques and the CFD-simulation method.

2 EXPERIMENTAL SETUP AND OPTICAL DIAGNOSTICS

A turbocharged 4-cylinder DI test engine with 1.4 l displacement and a central 6-hole injector was set up on a test bench. The engine was operated at an engine speed of 2,000 rpm, a boost pressure of 2.1 bar and a brake mean effective pressure of 21 bar.

A video access was installed on cylinder 4 to observe the initiation of pre-ignition. Two bores were applied to the cylinder head for the light source and the camera. High-speed imaging was carried out from two different directions by swapping camera and light source. No filters were used and the visible light content was above 350 nm.

As previously stated, pre-ignition frequently occurs within clusters of 3 to 5 events alternating with regular combustion cycles. The first observed pre-ignition of a cluster showed distinct differences in light-emissions to all following events: During the first pre-ignition cycle, a light source occurred spontaneously and immediately ignited the entire mixture. Due to the fact that there was no previous light emission, it is likely that the first pre-ignition was triggered by oil/fuel droplets that reached their critical condition for self-ignition at the moment when they became visible. Fig. 1 (a) shows an initial pre-ignition event.

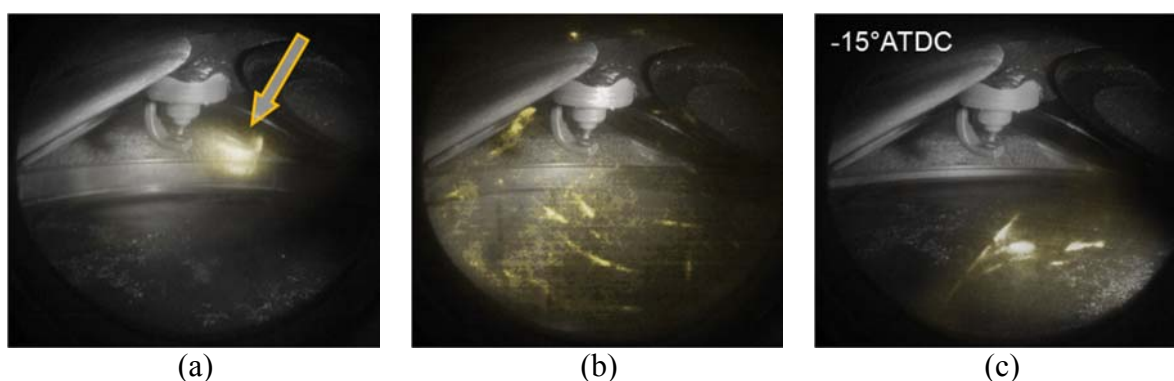


Figure 1: High-speed images of pre-ignition events: (a) Initial pre-ignition event; (b) Follow-up event with glowing particles; (c) Progress of one subsequent pre-ignition event due to a glowing particle

It was common to all pre-ignitions that in the following regular burning cycle glowing particles were observed, particularly during the final combustion phase, see Fig. 1 (b). Obviously, these particles are deposits. The videos suggest that some of these particles remain

in the combustion chamber and are heated up during the following regular combustion, where the time is sufficient for the heat transfer between gas and particle. Subsequent pre-ignitions are usually repeated 3 to 5 times until no major deposits were present in the combustion chamber.

2 SIMULATION OF THE WALL FILM FORMATION AND DROPLET TRACES

A CFD-simulation was carried out in order to analyse the wall film formation on the piston and the liner and hence the behaviour of droplets that are released from the film. Fuel components with high boiling temperatures were considered by introducing a multi-component surrogate fuel. Therefore, a simplified 0-dimensional calculation approach was developed to reproduce the measurement of the distillation curve according to DIN EN ISO 3405. During this procedure 100 ml of the fuel are electrically heated in a spherical distillation flask with a volume of 125 ml. The heating rate amounts 1 K/min. The vapour is afterwards condensed in a cooling pipe and collected in a measuring cylinder. For the simulation of the surrogate fuel's distillation curve the liquid in the distillation flask was assumed perfectly mixed, i.e. no temperature and concentration gradients occur. Following the work of Batteh and Curtis [5] the components ethanol, n-butane, isopentane, n-hexane, n-octane, 1,2,3-trimethyl-benzene, n-tridecane, 2,2,4 trimethyl-pentane and toluene were used to create a surrogate fuel with similar vaporization characteristics as the real fuel. Ideal liquid and ideal vapour was assumed in order to choose the same physics as it is implemented in the CFD-code. The mass flow \dot{m}_i of the different species from the liquid to the vapour phase was calculated referring to [5], see Eq. (1)

$$\dot{m}_i = Sh \cdot \left(\frac{p_i \cdot M_i}{\sum_j p_j \cdot M_j} \cdot \frac{A}{D/2} \cdot \rho_A \cdot \mathcal{D}_i \cdot \ln \frac{p_a}{p_a - p_v} \right) \quad (1)$$

where p_i denotes the partial pressure of species i and M_i the molecular weight. p_a is the ambient pressure and has the value 1 bar. ρ_A represents the ambient density and A is the free surface of the liquid. The concentration gradient above the liquid was assumed to be linear and is expressed by the radius of the distillation flask $D/2$. It is further assumed that the specific gas constant above the free surface equals the value of the fuel. The Ranz-Marshall-Correlation was used for the Sherwood number Sh , the vapour pressure p_v is the sum of the partial pressures p_i . Coefficients for the Antoine-equation were taken from [6], values for the diffusion coefficient \mathcal{D}_i from [7].

The mass fractions of the constituents were chosen to fit the measured distillation curve of the investigated fuel. Fig. 2 shows the adapted volume fractions of the five used components (right) tridecane, 1,2,3-trimethyl benzene, isooctane, n-hexane and isopentane as well as a comparison between the measured distillation curve and the calculated values (left).

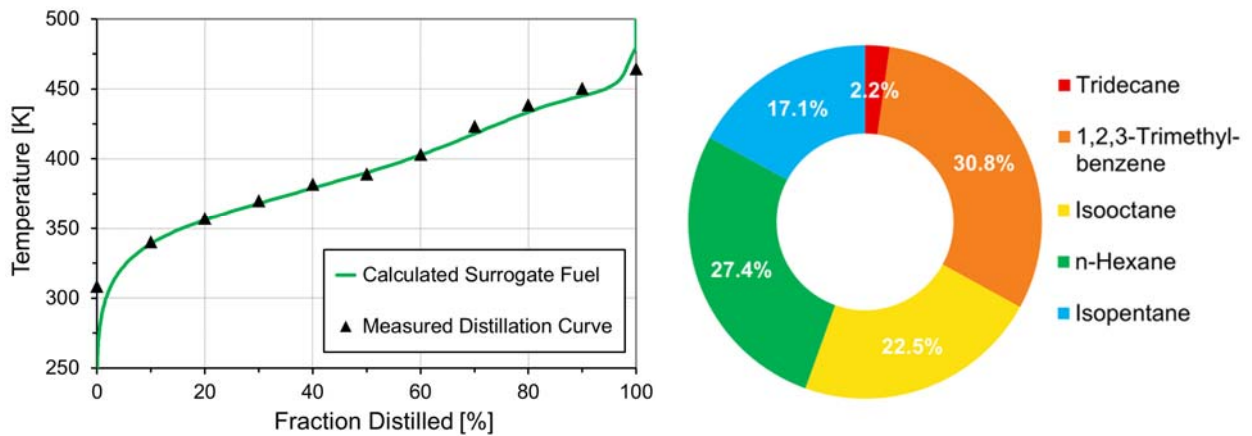


Figure 2: Distillation curve of the test bench fuel in comparison to the five-component model fuel (left) and the composition of the fuel components in vol-% (right)

The prediction of wall film formation on surfaces with a temperature in the range of the fluid's boiling temperature further requires a multi-regime impingement model that takes into account the wall temperature and the droplets' stability. In this work an adapted Bai-Gosman model was used [8]. The spray was modelled with a Lagrange-approach using the measured droplet spectrum as a boundary condition and the Reitz-Diwakar model for secondary break-up. The turbulent flow field was modelled with a 2-equation $k-\epsilon$ model. All simulations were carried out with Star-CD V4.18.

The simulation of an injection event revealed a distinct wetting of the piston crown under full load conditions already at a low engine speed. The spray is deflected by the intake flow's momentum and thus hits the piston crown in regions close to the liner, see Fig. 4. A mixing of fuel and lube oil and the accumulation of the fuel-oil-mixture in the piston crevice is therefore probable.

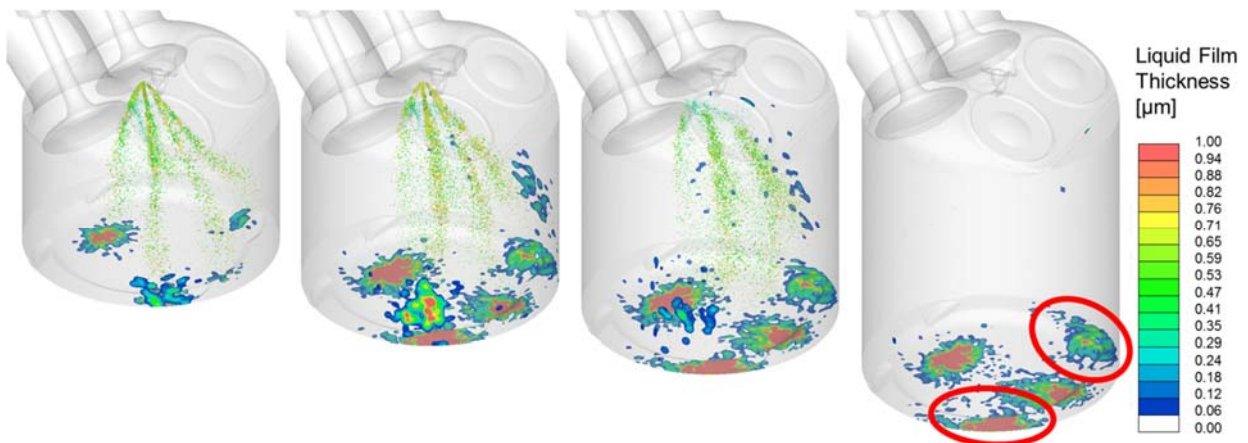


Figure 3: Formation of liquid film on the piston crown close to the liner (red circles) during intake stroke

The crevice volume was not modelled in detail. Therefore, droplets with an assumed diameter of $500 \mu\text{m}$ were released in regions with intensified wall wetting to mimic droplet stripping and the droplet traces in the combustion chamber, see Fig. 2. The trajectories were calculated up to the crank angle where the pre-ignitions were typically observed. A reasonable

correlation between the endpoints of the trajectories and the locations of pre-ignitions from the video observations (yellow symbols) could be found what supports the assumption of stripped droplets from wetted crevice areas as a source of pre-ignitions.

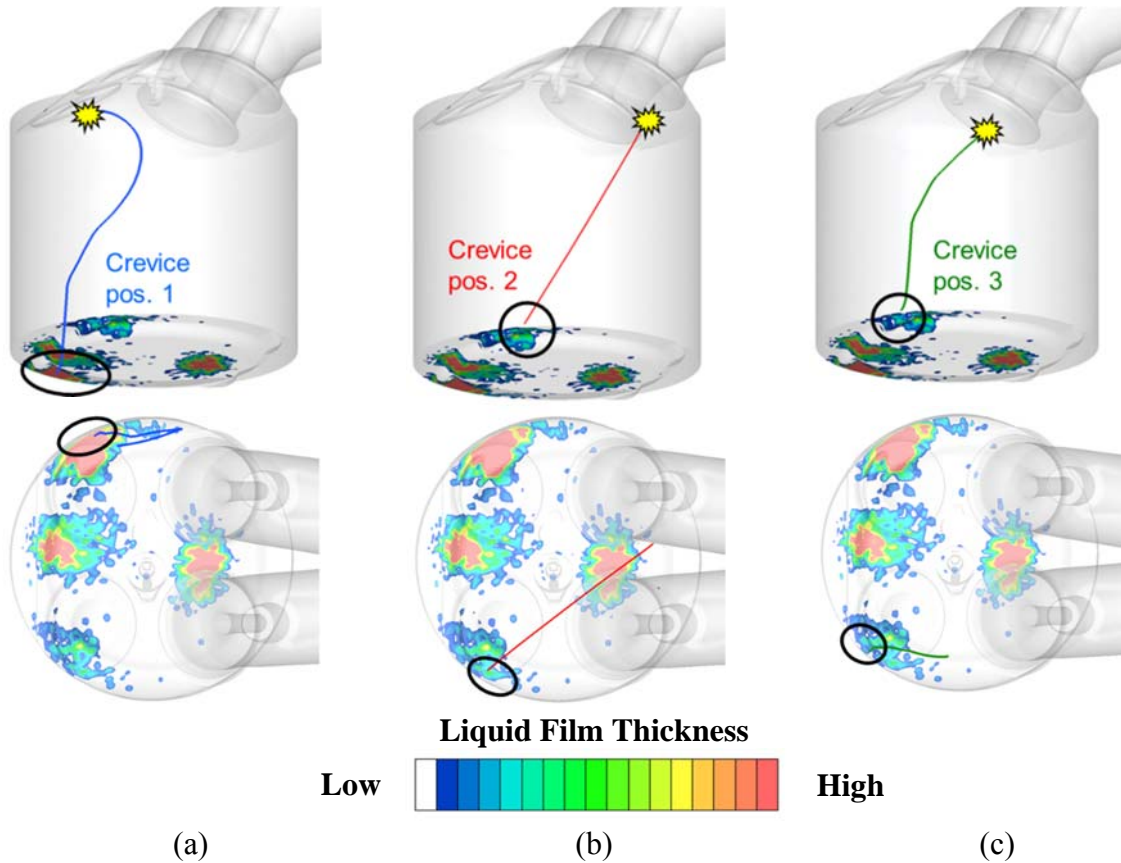


Figure 4: Trajectories of droplets (coloured lines) released from wetted crevice areas in comparison with recorded origins of pre-ignitions (yellow symbols)

3 INVESTIGATIONS ON FOLLOW-UP PRE-IGNITIONS

The optical investigations suggested that the follow-up pre-ignitions are triggered by glowing particles. They frequently occur after a regular combustion cycle. For a more elaborate analysis of the underlying mechanisms a multi-cycle CFD-simulation was carried out for the first pre-ignition, the following regular combustion cycle and the first follow-up pre-ignition. For the combustion a 3-zone enhanced coherent flame model was used. Its model parameters were adapted to the measured burn rates.

Particles were released after the first megaknock event from the discs of the exhaust valves and the crevice volume where a formation of solid deposits due to intensive wall wetting or high temperatures is likely. The release of the particles was assumed to take place during an interval of 5 °CA. The release timing (a) and the location (b) are illustrated in Fig. 5.

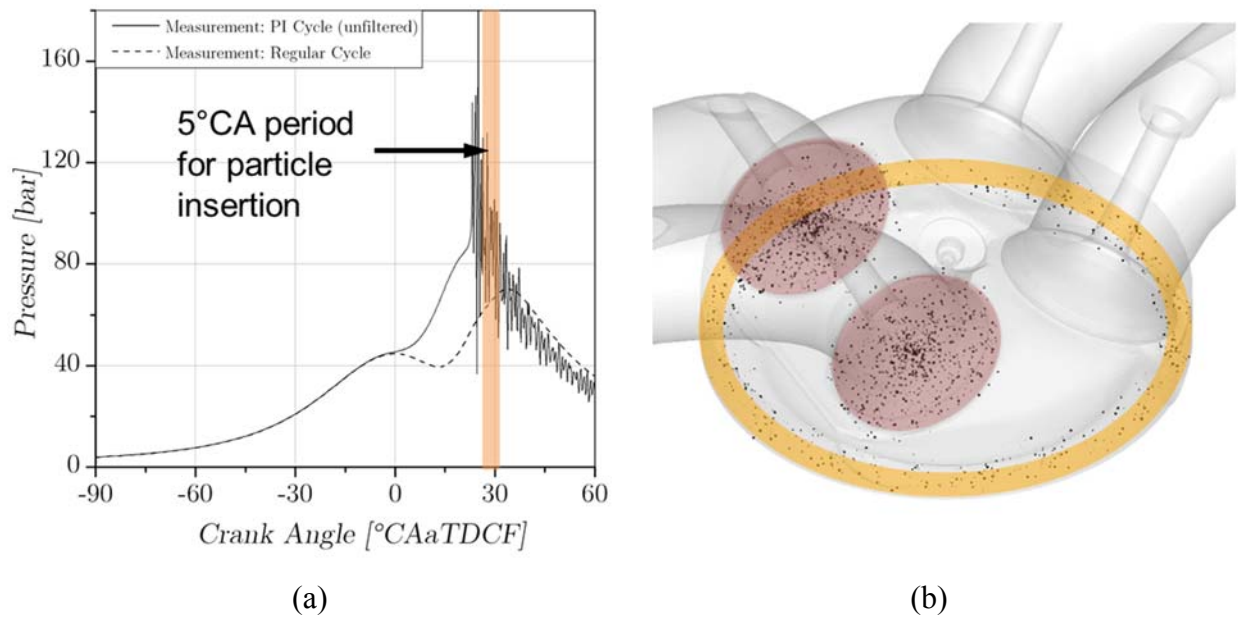


Figure 5: Timing (a) and regions (b) for particle insertion

The initial properties of the particles are summarized in Table 1. Their initial speed after being detached by the pressure oscillations of the megaknock event and their diameter has been varied to study the impact of both parameters on their further behaviour. The particles' initial temperature was chosen to a typical cylinder wall temperature.

Table 1: Specification of inserted particles

| | |
|--------------|--|
| Total number | 6,000 particles |
| Diameter | $50 \mu\text{m} \leq d \leq 500 \mu\text{m}$ |
| Velocity | $0 \text{ m/s} \leq v_{\text{init}} \leq 10 \text{ m/s}$ |
| Temperature | 500 K |

The following Fig. 3 shows the number of particles that remain inside the combustion chamber during the two calculated exhaust strokes, i.e. until the first follow-up pre-ignition event occurs. For a better visualisation the cylinder pressure is included on the second ordinate. The opening of the exhaust valves is illustrated with shaded bars.

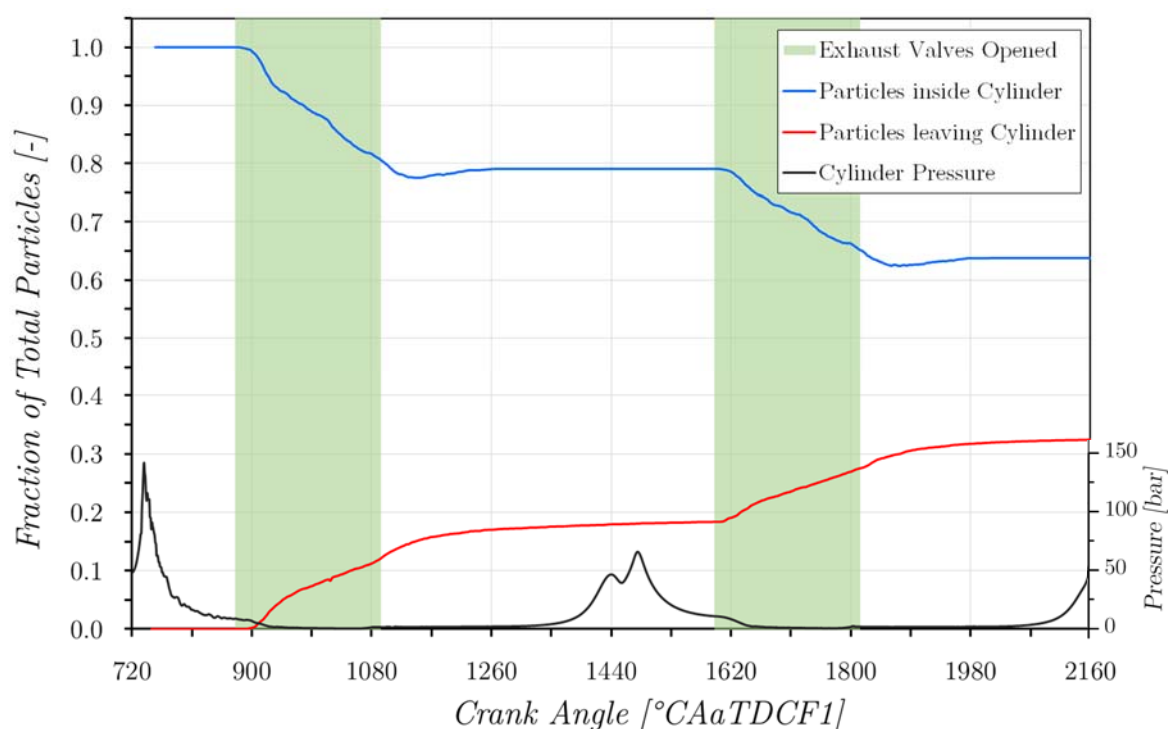


Figure 6: Evolution of the number of particles over 3 cycles

It becomes obvious that more than 60 % of the originally released particles remain in the combustion chamber. It could be further shown that a disproportionately high amount of small particles leave the combustion chamber whereas the bigger particles rather remain in the combustion chamber what can be argued with the fact that the bigger particles do not follow the flow field instantaneously due to their higher inertia. This outcome is qualitatively in a good agreement with the observations at the engine test bench.

In order to study the heating and the thermal inertia of the particles the properties of solid soot were assigned. The particles were estimated as spherical and no temperature distribution and no exothermal reactions were considered. Their trajectories were solved with a Lagrange approach.

It could be shown with this simplified method that the small particles are immediately heated above the self-ignition temperature of soot that was assumed to be 900 K. Therefore, it is likely that they are burned immediately after the first pre-ignition. Fig. 7 shows typical temperature curves for particles with diameters up to 165 μm . Additionally, the self-ignition limit of soot is added to the diagram.

Due to the fact that no exothermic reactions are modelled, what is a severe simplification, the particles do not disappear after reaching a temperature beyond the self-ignition point of soot. However, it can be assumed that they burn quickly if a sufficient oxygen concentration prevails in the combustion chamber. Therefore, their traces are marked with dashed lines after inlet valve opening indicating that they are burnt.

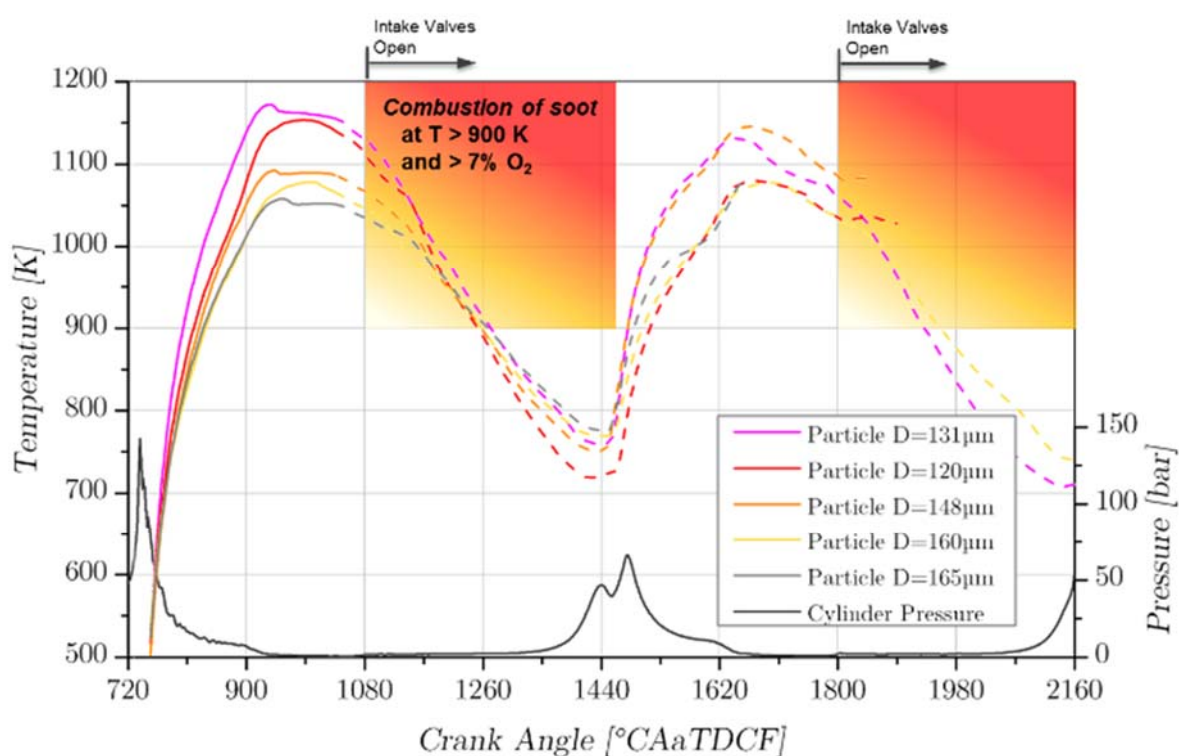


Figure 7: Temperature history of the hottest particles at compression start of the 2nd cycle

In addition, the investigations revealed that the bigger particles significantly increase in temperature during the regular burning cycle and distinctly exceed the self-ignition limit. In Fig. 8, the temperature curves of the five hottest particles are plotted.

Though no exothermic reactions were considered it becomes clear that the temperature of the particles increase steadily if they survive the exhaust stroke of the first pre-ignition event. During the regular combustion, the crank angle range to heat the particles is bigger than for the first pre-ignition cycle. This leads to particle temperatures that exceed the temperatures after the first pre-ignition by approx. 200 K. These results suggest that during the regular combustion most particles are ignited. Due to their size they are likely to survive the following exhaust and inlet stroke and ignite the mixture during compression at sufficiently high mixture temperatures. Therefore, the observation of an alternating succession of cycles with pre-ignition and regular combustion can be explained with the intensive heating of the remaining particles during the regular combustion.

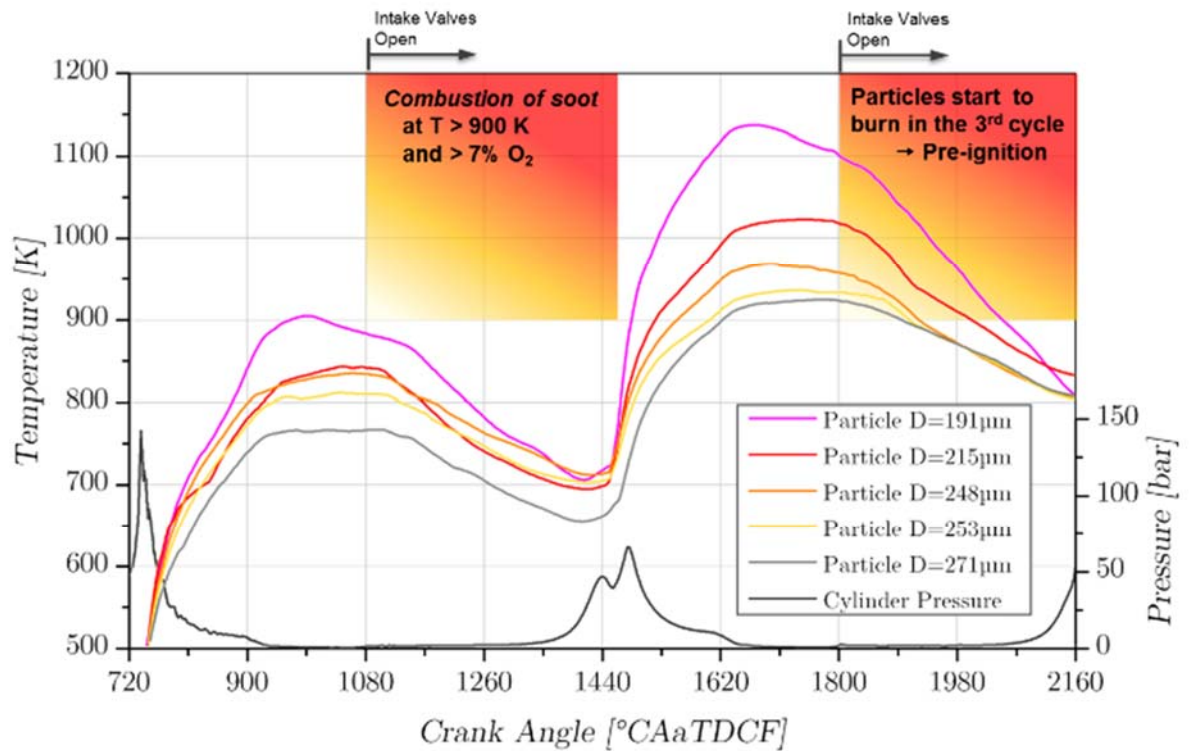


Figure 8: Temperature history of the hottest particles at compression start of the 3rd cycle

4 CONCLUSIONS

CFD-simulations were carried out in order to explain the underlying mechanisms to pre-ignition events and their alternating occurrence at the test bench.

It could be confirmed that the stripping of droplets and the detachment of deposits are possible causes for pre-ignitions. However, further model enhancements like the exothermic reactions on the particles' surfaces must be considered what could be the content of future work.

REFERENCES

- [1] Takeuchi, K.; Fujimoto, K.; Hirano, S.; Yamashita, M.: Investigation of Engine Oil Effect on Abnormal Combustion in Turbocharged Direct Injection - Spark Ignition Engines. In: SAE Technical Paper: 2012-01-1615
- [2] Yasueda, S.; Takasaki, K.; Tajima, H.: Abnormal Combustion caused by Lubricating Oil in High BMEP Gas Engines. In: MTZ Industrial (2013), Vol. 3, pp. 34-39
- [3] Zahdeh, A.; Rothenberger, P.; Nguyen, W.; Anbarasu, M.; Schmuck-Soldan, S.; Schaefer, J.; Goebel, T.: Fundamental Approach to Investigate Pre-Ignition in Boosted SI Engines. In: SAE Technical Paper: 2011-01-0340
- [4] Lauer, T.; Heiß, M.; Bobicic, N.; Holly, W.; Pritze, S.: A Comprehensive Simulation Approach to Irregular Combustion. SAE Technical Paper 2014-01-1214
- [5] Batteh, J. J.; Curtis, E. W.: Modeling Transient Fuel Effects with Alternative Fuels. In: SAE Technical Paper: 2005-01-1127
- [6] National Institute of Standards and Technology: www.nist.gov – February 2012
- [7] VDI-Gesellschaft Verfahrenstechnik und Chemie-Ingenieurwesen (GVC): VDI-Wärmeatlas – Berechnungsblätter für den Wärmeübergang. 5. Auflage, Düsseldorf: VDI-Verlag, 1988
- [8] Heiss, M.; Lauer, T.: Simulation of the Mixture Preparation for an SI Engine using Multi-Component Fuels. STAR Global Conference 2012, Amsterdam: 2012